LU TP 93-27

Heavy Quark Production in Jets

M.H. Seymour
Department of Theoretical Physics, University of Lund,
Sölvegatan 14A, S-22362 Lund, Sweden

Abstract

We discuss the Monte Carlo simulation of heavy quark production in high-p_t jets. An algorithm is described that allows such rare processes to be studied in a realistic amount of computer time. The results of the algorithm are compared with analytical calculations for a colour-singlet source, and presented for the first time for hadron-hadron collisions.

LU TP 93-27
November 1993

LU-TP-93-27
Fermilab Library
0 1160 0034441 0

1 Introduction

The production of heavy quark pairs at high p_t is a good test of perturbative QCD, since the quark mass, m_q, provides a natural infrared cutoff. Therefore a perturbative expansion in $\alpha_s(m_q)$ is expected to give a reliable estimate of the heavy quark cross-section. Furthermore, when the p_t is much larger than the quark mass, the cross-section is dominated by logarithms of p_t/m_q, which are independent of the production mechanism of the associated jet. It then makes sense to discuss the ***multiplicity*** of heavy quarks within the jet rather than their cross-section, since all dependence on the parton distribution functions and hard process cross-sections then disappear, leaving a quantity that is fully calculable in perturbation theory[1]. The leading non-perturbative corrections were calculated in [2] and found to be small.

However, because the logarithmic terms are large, and appear at all orders in the expansion in $\alpha_s(m_q)$, they must be reorganised into an improved perturbation series that resums all large terms in the original series. This is most easily done in terms of evolution equations that describe how the quantity of interest changes with jet scale (for a review, see [3]). In [4], the multiplicities for any parton species inside a jet of any species were derived to next-to-leading logarithmic accuracy (i.e. resumming all terms of the form $\alpha_s^n \log^m$, $m = 2n, 2n-1$), while in [5] a slightly different approach was used for the specific case of heavy quark pairs.

Another approach to resumming large logarithms is to formulate the evolution as a probabilistic chain, which can be simulated numerically using Monte Carlo methods[6–9]. Such algorithms are generally only to leading logarithmic accuracy, but include many important additional effects, such as energy-momentum conservation, which only enters analytical calculations at next-to-next-to-leading order[10]. They have been extremely successful in describing experimental data in terms of a small number of adjustable parameters, particularly in the relatively well-understood environment of e^+e^- annihilation into hadrons.

The Monte Carlo algorithms currently in use have a common feature that they simulate jets with unit weight. That is, they produce jet configurations with the same frequency as in nature. When studying rare processes, such as heavy quark production, this is a considerable problem since many events must be generated, most of which are never used. This even makes some studies impossible, because of the amount of computer time they would require.

In this paper we describe an algorithm capable of producing jets with any required flavour configuration (or indeed scale configuration, although we do not discuss that here). The key new feature relative to the HERWIG algorithm, of

which it is a development, is the ability to calculate the relative probability of generating any given flavour/momentum configuration in a closed form. This requires the explicit calculation of all the relevant form factors, and the removal of so-called vetoes in the generation of the scale of each branching. The latter requirement is rather strict, and means that any algorithm that relies heavily on such vetoes cannot be improved in the way described here.

The remainder of the paper is set out as follows. In Sect. 2 we describe the Monte Carlo algorithm, paying particular attention to the explicit calculation of the form factors. We give results for the bottom quark multiplicity in gluon and quark jets produced by colour-singlet sources, and discuss some of the approximations made. In Sect. 3 we discuss the analytical results of [4], and compare them with the method of [5], and with the Monte Carlo results. We also propose a modification to the result for a quark jet that makes no difference within the next-to-leading logarithmic approximation in which it is valid, but gives a result that is more physically reasonable owing to a change in the sub-leading terms. Finally in Sect. 4 we discuss the application of our algorithm to hadron-hadron collisions, and give the results for the p_t spectrum of bottom quark pairs in proton-antiproton collisions at $\sqrt{s} = 1.8$ TeV.

Our algorithm is implemented as a package of additional routines for HERWIG, and is available by emailing the author, `mike@thep.lu.se`.

2 Monte Carlo Algorithm

In perturbation theory, large logarithms arise in the cross-section for multi-parton final states owing to configurations where two or more partons become almost collinear. To accurately determine such cross-sections, these logarithms must be resummed to all orders. This resummation can be formulated as an iterative procedure, such that individual phase-space contributions can be simulated using Monte Carlo algorithms[6–9]. Such algorithms are capable of describing many of the gross features of hard scattering events and, together with hadronisation models[11,12], more specific features of their hadronic final states.

The large logarithms associated with soft gluon radiation can also be resummed in a Monte Carlo algorithm, by appropriate choice of the evolution variable. This follows from the coherence of the soft gluon radiation, which reduces the multi-gluon phase-space to the angular-ordered one, after azimuthal averaging. That is, it can be described as a factorised series of branchings, each with an opening angle smaller than the last. In the HERWIG algorithm[6], this

is done by defining the evolution variable to be

$$Q^2 \equiv E^2\xi \equiv E^2\, p_i{\cdot}p_j\, / E_i E_j \approx E^2(1-\cos\theta_{ij}), \tag{1}$$

where $E = E_i + E_j$ and $E_{i,j}$, $p_{i,j}$ are the energies and 4-momenta of the two produced partons. The final approximation becomes exact when the produced partons are massless. It can immediately be seen that ordering in Q^2 corresponds to ordering in opening angle.

A central rôle in any branching algorithm is played by the form factor, $\Delta(Q^2)$, defined as the probability that a parton capable of branching at scales up to Q^2 does not produce any resolvable radiation. This can be written in terms of the naïve probability that it does radiate,

$$\Delta(Q) = \exp\left\{-\int_{Q_c}^{Q}\frac{dk}{k}\int_{z_i(k)}^{1-z_j(k)} dz P(z)\frac{\alpha_s}{\pi}\right\}, \tag{2}$$

where z is the energy-fraction of the splitting, and Q_c and $z_{i,j}$ are infrared cutoffs to be defined shortly. We shall also make use of the two-scale form factor,

$$\Delta(Q,q) \equiv \frac{\Delta(Q)}{\Delta(q)} = \exp\left\{-\int_{q}^{Q}\frac{dk}{k}\int_{z_i(k)}^{1-z_j(k)} dz P(z)\frac{\alpha_s}{\pi}\right\}. \tag{3}$$

For gluon emission, the infrared cutoff is on the local transverse momentum of the emission. Kinematically, this gives us

$$z_i(k) = Q_i/k, \tag{4}$$

where Q_i is the cutoff for parton type i. Coherence in heavy quark fragmentation can also be incorporated by careful choice of Q_i. This coherence results in an emission probability that is identical to that of a light quark at large angles, but is suppressed within a cone of opening angle m_q/E_q, the 'dead cone'. Kinematically, this is achieved by $Q_q \sim m_q$. We set

$$Q_q = Q_0 + m_q, \tag{5}$$

where Q_0 is a flavour-independent parameter of the model, which has a tuned value of order 500 MeV. The cutoff Q_c is simply given by the point where $z_i + z_j = 1$, that is,

$$Q_c = Q_i + Q_j. \tag{6}$$

In the $\overline{\mathrm{MS}}$ scheme, the splitting of a gluon to massive fermions is identical to the splitting to massless ones above threshold, and zero below. This corresponds to setting $z_q = 0$ when considering $\mathrm{g} \to \mathrm{q\bar{q}}$, but retaining $Q_c = 2Q_q$.

Many of the next-to-leading logarithmic terms can be resummed by suitable treatment of the running coupling. Indeed by using as its scale the relative transverse momentum of emission, and its two-loop running form,

$$\alpha_s = \alpha_s^{(2)}(z(1-z)k), \tag{7}$$

a precise connection can be made between the HERWIG scheme and the $\overline{\mathrm{MS}}$ scheme, at least in the semi-inclusive region, $x \to 1$[13]. This means that the Λ_{QCD} in HERWIG has a precise relationship with $\Lambda_{\overline{\mathrm{MS}}}$, rather than being a freely adjustable parameter. For gluon splitting to quarks there are no soft logarithms to resum, and the scale used for α_s should be k.

The differential probability for the first splitting of a parton with upper scale Q to be at scale q is then given by

$$d\mathcal{P}(q;Q) = \frac{dq}{q}\int_{z_i(q)}^{1-z_j(q)} dz P(z)\frac{\alpha_s}{\pi}\Delta(Q,q) = d\Delta(Q,q). \tag{8}$$

Since the right-hand side is a total integral, q values can be generated with this distribution simply by choosing a uniform random number on the range $[0,1]$, ρ, and solving

$$\rho = \Delta(Q,q) \tag{9}$$

in q. If this solution is above Q_c, then it corresponds to emission at scale q. Otherwise there was no resolvable emission and the algorithm terminates. This can be easily generalised to the case of more than one type of competing branching, by choosing q values corresponding to each type of branching according to the above procedure, and then using the largest.

If $\Delta(Q,q)$ is not a conveniently invertible function, a trick known as the veto algorithm can be used. This involves finding a function Δ' that is invertible and has a derivative that is everywhere larger than that of Δ. One then generates q according to Δ', and vetoes a fraction $d\Delta(q)/d\Delta'(q)$ of these emissions (i.e. the chosen emission is not considered resolvable, and the evolution continues from the chosen scale). However, the improvement to the algorithm that we describe here relies on knowing the form factor in a closed form, and so we should avoid using vetoes where possible. In some algorithms[9], vetoes are also used to enforce kinematic constraints. Since these usually have an uncalculable effect on the form factor, such algorithms cannot be improved in the way we describe here. As we discuss below, one such veto exists in HERWIG for extreme kinematic configurations, which slightly reduces the efficiency of our algorithm.

2.1 Gluon emission form factor

The splitting functions are

$$P_{q\to qg}(z) = C_F\frac{1+(1-z)^2}{z}, \tag{10}$$

$$P_{g\to gg}(z) = C_A\frac{1+z^4+(1-z)^4}{z(1-z)}, \tag{11}$$

where $C_A = N_c = 3$ and $C_F = (N_c^2-1)/2N_c = 4/3$. Exchanging the order of integration relative to (2), we obtain

$$-\log\Delta(Q) = \int_{Q_i/Q}^{Q_i/Q_c} dz P(z)\int_{Q_i/z}^{Q}\frac{dk}{k}\frac{\alpha_s(z(1-z)k)}{\pi} + (i\leftrightarrow j,\ z\leftrightarrow(1-z)). \tag{12}$$

The inner integral can be performed by using the second order renormalisation group equation,

$$\mu^2\frac{d\alpha_s}{d\mu^2} = -\beta_0\alpha_s^2(1+\beta'\alpha_s), \tag{13}$$

where the β coefficients are functions of the number of flavours considered to be light at scale μ, f,

$$\beta_0 = \frac{1}{12\pi}(11C_A - 2f), \tag{14}$$

$$\beta' \equiv \frac{\beta_1}{\beta_0} = \frac{1}{24\pi^2\beta_0}(17C_A^2 - (5C_A+3C_F)f). \tag{15}$$

This can be used to rewrite the integral

$$\int\frac{dk}{k}\frac{\alpha_s(\mu)}{\pi} = \sum_f\frac{1}{2\pi\beta_0}\left[\log\frac{1}{\beta'+1/\alpha_s}\right]_{\alpha_s(\min(z(1-z)Q,m_{f+1}))}^{\alpha_s(\min((1-z)Q_i,m_f))}, \tag{16}$$

where the sum over f accounts for the flavour thresholds. The final integral, over z, is calculated and inverted numerically in HERWIG, to generate the distribution of q.

2.2 Gluon splitting form factor

The splitting function is

$$P_{g\to q\bar{q}}(z) = \tfrac{1}{2}(z^2+(1-z)^2). \tag{17}$$

Thus the form factor is given by

$$\Delta(Q) = \exp\left\{-\int_{2Q_q}^{Q}\frac{dk}{k}\int_0^1 dz(z^2+(1-z)^2)\frac{\alpha_s(k)}{2\pi}\right\} \tag{18}$$

$$= \exp\left\{\frac{-1}{3\pi}\int_{2Q_q}^{Q}\frac{dk}{k}\alpha_s(k)\right\} \tag{19}$$

$$= \left(\frac{\beta'+1/\alpha_s(2Q_q)}{\beta'+1/\alpha_s(Q)}\right)^{\frac{1}{6\pi\beta_0}}. \tag{20}$$

Again, the flavour thresholds can be incorporated by writing the integral as a sum over flavours,

$$\Delta(Q,2Q_q) = \Delta(Q,m_f)\Delta(m_f,m_{f-1})\ldots\Delta(m_{q+1},2Q_q). \tag{21}$$

The two-scale form factor can then be inverted to generate q, by first finding the flavour region, n, in which the solution lies, and then solving

$$\left(\frac{\beta'+1/\alpha_s(q)}{\beta'+1/\alpha_s(Q)}\right)^{\frac{1}{6\pi\beta_0}} = \rho \qquad \text{if } n=f, \tag{22}$$

$$\left(\frac{\beta'+1/\alpha_s(q)}{\beta'+1/\alpha_s(m_{n+1})}\right)^{\frac{1}{6\pi\beta_0}} = \rho\frac{\Delta(m_{n+1},2Q_q)}{\Delta(Q,2Q_q)} \quad \text{otherwise}, \tag{23}$$

in $\alpha_s(q)$, and inverting this to find q.

2.3 Forcing quark pair production

Once we have the form factor for each type of branching in a closed form like this, we can force the first heavy quark pair to be produced at the nth branch, simply by switching off $g \to q\bar{q}$ during the first $n-1$ branchings, and switching off $g \to gg$ at the nth. At each stage, the branching is required to be resolvable. We neglect the effect of light quark production, and discuss this approximation in a later section. A weight factor is then assigned to the jet as a whole, which is the products of the probabilities of each stage that we have forced. That is, the probability of having the nth gluon splitting producing the first heavy quark pair at scale q_n, with each of the intervening splittings at scales q_i is

$$\mathcal{P}_n(q_1,\ldots,q_n) = \prod_{i=1}^{n-1}(1-\Delta_{gg}(q_{i-1},2Q_g))\,\Delta_{q\bar{q}}(q_{i-1},q_i) \times(1-\Delta_{q\bar{q}}(q_{n-1},2Q_q))\,\Delta_{gg}(q_{n-1},q_n), \tag{24}$$

with $q_0 \equiv Q$. Both lines should also be multiplied by the form factors of any other types of emission that are switched off, for example gluon splitting to light quarks or, in some models, diquarks.

As a specific example, consider $n=3$. We first produce two gluons at scales $q_{1,2}$, and energy fractions $z_{1,2}$, which are forced to be inside the phase-space, and before any quark splittings. Then we produce a heavy quark pair at scale q_3, which is again forced to be inside the phase-space, and before a third gluon is emitted. Thus the combined probability for each stage we have forced is

$$\begin{aligned}\mathcal{P}_3(q_1,q_2,q_3) &= (1-\Delta_{gg}(Q,2Q_g))\,\Delta_{q\bar{q}}(Q,q_1)\\ &\times (1-\Delta_{gg}(q_1,2Q_g))\,\Delta_{q\bar{q}}(q_1,q_2)\\ &\times (1-\Delta_{q\bar{q}}(q_2,2Q_q))\,\Delta_{gg}(q_2,q_3).\end{aligned} \tag{25}$$

The first term of the first line is the probability that a gluon is emitted between Q and $2Q_g$, the second term is the probability that no quarks are emitted between Q and q_1, i.e. before the first gluon, and likewise for the subsequent lines.

2.4 Reduced phase-space for gluons

If we wish to force heavy quark pair production at a given vertex of the shower, we must ensure that earlier emissions leave enough phase-space for it. With the angular-ordered kinematics, this gives a simple modification of the infrared cutoff—it is replaced by the sum of the cutoffs for all particles that must be produced. So for a heavy quark pair to be produced n emissions later than the one we are considering, $(n-2)Q_g+2Q_q$ must be added to the cutoff. For gluons this leaves a cutoff of

$$Q_n = (n-1)Q_g + 2Q_q, \tag{26}$$

with obvious generalisation to the quark case (where $n=1$ is not allowed by conservation of baryon number). The probability distribution for the first gluon emission below Q to be at q, with enough room for the subsequent splitting is then

$$d\mathcal{P}(q;Q) = \frac{dq}{q}\int_{Q_n/q}^{1-Q_g/q} dz P(z)\frac{\alpha_s}{\pi}\exp\left\{-\int_q^Q\frac{dk}{k}\int_{Q_g/q}^{1-Q_g/q} dz P(z)\frac{\alpha_s}{\pi}\right\}. \tag{27}$$

Note that the reduced phase-space appears in the first term, representing the probability that the actual emission is in the phase-space, while the full phase-space appears in the form factor, since competing radiation need only be resolvable. Defining the modified form factor,

$$\Delta'(Q,q) = \exp\left\{-\int_q^Q\frac{dk}{k}\int_{Q_n/k}^{1-Q_g/k} dz P(z)\frac{\alpha_s}{\pi}\right\}, \tag{28}$$

this probability distribution can be written as

$$d\mathcal{P}(q;Q) = d\Delta'(Q,q)\frac{\Delta(Q,q)}{\Delta'(Q,q)}. \tag{29}$$

In other words, one can generate q by inverting the modified form factor, and then weight the event by the ratio of two-scale form factors at that point.

2.5 Improving the efficiency

Clearly the q distribution of the first branching of a jet that produces a quark-antiquark pair at its nth branching, is not the same as that of a general jet. In particular, near to threshold the distribution can be pushed towards much higher q values. We can incorporate some of these effects by a simple modification of the generated distribution, bearing in mind that we may only use distributions that can be integrated analytically, so an exact reweighting (which could be implemented using the veto algorithm) is not possible.

For gluon splitting to quarks, the contribution of a given vertex to the overall weight is given by

$$d\mathcal{P}(q;Q) = d\Delta_{q\bar{q}}(Q,q)\,\Delta_{gg}(Q,q). \tag{30}$$

To leading order, with fixed coupling, it is easy to show that $\Delta_{q\bar{q}}(Q,q)$ and $\Delta_{gg}(Q,q)$ can be related by a simple power law,

$$\Delta_{gg}(Q,q) = (\Delta_{q\bar{q}}(Q,q))^a\,, \tag{31}$$

with a a calculable constant. Empirically, graphs of $\log\Delta_{gg}(Q,q)$ as a function of $\log\Delta_{q\bar{q}}(Q,q)$ are reasonably straight even for Q values as large 50 TeV. Furthermore, they are guaranteed to be concave upwards, that is the straight line joining their endpoints is everywhere above the actual curve. This makes this straight line an ideal Monte Carlo distribution to generate, including the appropriate weight in the integral.

That is, instead of generating $\Delta_{q\bar{q}}(Q,q)$ uniformly as usual, we generate

$$d\Delta_{q\bar{q}}(Q,q)\,(\Delta_{q\bar{q}}(Q,q))^a\,, \tag{32}$$

$$a = \frac{\log\Delta_{gg}(Q,2Q_q)}{\log\Delta_{q\bar{q}}(Q,2Q_q)}. \tag{33}$$

a ranges from around 50 for $Q = 20$ GeV, to 200 for $Q = 50$ TeV. The Jacobian factor appearing in the overall weight then reads

$$\frac{1}{a+1}\left(1-(\Delta_{q\bar{q}}(Q))^{a+1}\right)\frac{1}{(\Delta_{q\bar{q}}(Q,q))^a}. \tag{34}$$

As an example, for the first $b\bar{b}$ emission from a 1 TeV gluon jet, this increases the Monte Carlo efficiency from 9% to 64%.

A similar procedure is also possible for the case of gluon emission within the reduced phase-space, but with a replaced by

$$a = \left.\frac{d\log\Delta_{gg}(Q,q)}{d\log\Delta_{q\bar{q}}(Q,q)}\right|_{q=Q}, \tag{35}$$

since the equivalent graphs are convex.

2.6 Combinatorial factors

The above procedure is capable of simulating jets that produce a heavy quark pair at a given vertex, but to complete the algorithm we must also choose for each event, which vertex of which jet will produce the pair. This must also account for the (small) probability that an event will contain more than one pair.

Having decided that the pair is to be produced at the nth vertex of a jet, we must sum over the different jet configurations in which this occurs. Neglecting the effect of internal light quark lines, this is simple; for gluon-initiated jets there are 2^{n-1} symmetric configurations, which have equal weight. For quark-initiated jets, there is one less configuration, owing to the absence of a $q \to Q\bar{Q}$ vertex, and they are no longer symmetric. However, we find empirically that each configuration has similar weight, so we generate equal numbers of each.

Within a single jet, the average weight for pairs to be produced at the nth vertex is roughly constant with n, although a better estimate of this is an area in which the efficiency could be improved. We generate equal numbers of events with n in the range 1 to N. By default, N is set to the integer nearest to $1+\log(Q^2/4m_q^2)$, an empirical limit that can be overridden by the user if necessary. The possibility of several pairs being produced at different values of n is easily incorporated by switching off production of the requested heavy quark pair at all vertices before n, but simulating the jet as normal after n. The possibility of several pairs being produced at the same n is not as simple; to avoid double-counting we cannot just allow other pairs to be produced at the same depth in the shower with their natural weight. Instead, we usually switch off the heavy quark production at the other vertices, and in a small fraction of events explicitly generate more than one pair.

A similar combinatorial problem exists when there is more than one jet consider. We first estimate the probability that each jet will contain quark pair using the analytical result discussed in the next section. The

these estimates, we can calculate the probability that any given combination of jets contains heavy quark pairs. To illustrate the idea, consider the case of two jets. If our estimates of the probability that each jet will contain a pair are p_1 and p_2, then we estimate that the probability of both is $p_1 p_2$. Thus, a fraction

$$f_i = \frac{p_i}{p_1 + p_2 + p_1 p_2} \tag{36}$$

of the time we choose jet i only to produce the pair, and a fraction

$$f_{12} = \frac{p_1 p_2}{p_1 + p_2 + p_1 p_2} \tag{37}$$

of the time we choose both. In each case, we multiply the corresponding weight factor by $1/f$. To avoid double counting, the heavy quark pair production must be switched off during the first N vertices of any jets that were not chosen. A similar algorithm applies when there are more than two jets.

Note that all the assumptions we make in this section, such as the constancy of the weight with depth within the jet, only affect the efficiency of the Monte Carlo algorithm, and not the actual distribution of events produced. Since we calculate the weight of each configuration as we produce it, the assumptions we make about the weight distribution are always corrected for in the output distributions.

2.7 Results

In Fig. 1, we show the multiplicity of bottom quark pairs in a gluon jet as a function of its hardness, Q (strictly speaking, this is half the multiplicity in events in which gluon pairs are produced in a colour-singlet state of invariant mass $\sqrt{2}Q$). It begins to rise logarithmically from threshold, as would naïvely be expected, and then increases more rapidly as the parton multiplication takes off at $Q \sim (2Q_q)\exp(1/\sqrt{\alpha_s}) \sim 300$ GeV.

Also shown are the individual contributions from each vertex of the parton shower, which never rise much above one percent.

The Monte Carlo efficiency of our algorithm is also shown. It is extremely high at low energy, but decreases with energy until at $Q \sim 1$ TeV it crosses the solid line, meaning that our algorithm gives no improvement over the standard method.

In Fig. 2, we show the equivalent curves for a quark jet (again defined as half of a colour-singlet event). Its features are qualitatively similar except that it rises slowly from threshold, as would be expected from the absence of a $q \to Q\bar{Q}$

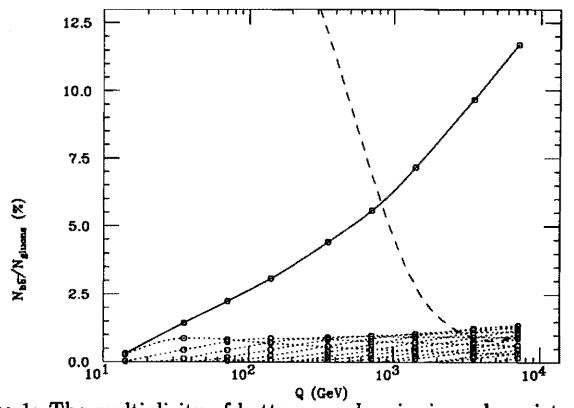

Figure 1: The multiplicity of bottom quark pairs in a gluon jet as a function of the jet hardness, Q (solid), together with the individual contributions from each vertex (dotted), and the Monte Carlo efficiency of event generation (dashed).

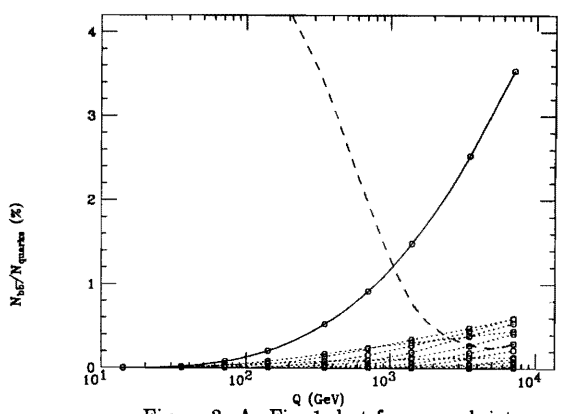

Figure 2: As Fig. 1, but for a quark jet.

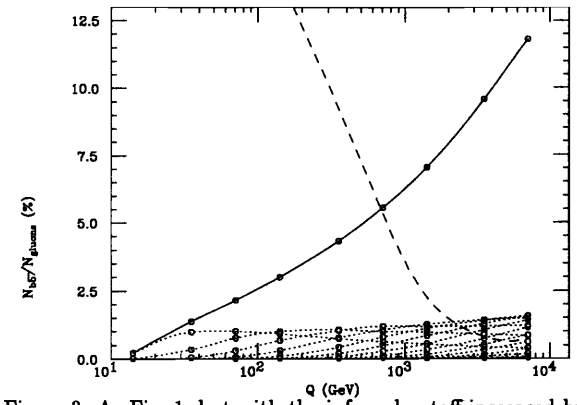

Figure 3: As Fig. 1, but with the infrared cutoff increased by 500 MeV.

One interesting test of our algorithm is its infrared safeness. As mentioned in the introduction, this is one of the reasons for interest in heavy quark production in jets. The curves corresponding to emission at each vertex of the jet are certainly infrared sensitive, since changing the cutoff on gluon emission will change the number of resolvable gluons emitted at angles larger than the heavy quark opening angle. However, their sum should be infrared safe, and thus invariant under changes of this cutoff. In fact small violations would be expected because HERWIG assigns a mass to the gluon and conserves energy at each vertex. As shown in Fig. 3 this effect is small, and the total multiplicity is, to a good approximation, infrared safe.

2.8 Approximations

The only approximations we have made, relative to the standard HERWIG algorithm, are to truncate the emission after N vertices, and to neglect the effect of internal light quarks. The effect of the former can be seen in Figs. 1 and 2—the default value, $N \approx 1 + \log(Q^2/4m_q^2)$, is perfectly adequate.

Although we do not have an algorithm that systematically sums over all jet configurations that include light quarks, it is easy to include the first contribution, $n = 3$, since it only has two symmetrical configurations, i.e. $g \to q\bar{q} \to q\bar{q}g \to q\bar{q}Q\bar{Q}$. In Fig. 4 we show the ratio of this process to the dominant $n = 3$ one, $g \to \ldots \to ggQ\bar{Q}$. The combinatorial factors from the sum over configurations (1/2) and light flavours (4) are included. It can be seen that the light quark contribution is always less than one percent of the gluon contribution, and is

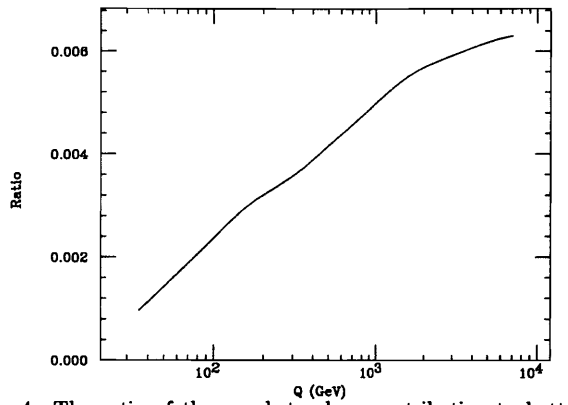

Figure 4: The ratio of the quark to gluon contribution to bottom quark pair production in a gluon jet at the third vertex.

therefore negligible. However, we note that parton mixing is formally a next-to-leading logarithmic correction, and thus such effects would have to be included if a full next-to-leading Monte Carlo prescription were attempted.

3 Analytical Results

The resummed multiplicities of one parton type within another were calculated to next-to-leading logarithmic accuracy in [4]. Their results for the quark multiplicity are

$$\mathcal{N}_q^q(Q_0, Q) = \mathcal{N}^-(z_0, z_1) + \frac{8}{3}\frac{C_F}{C_A}\frac{n_f}{b}\tilde{\mathcal{N}}(z_0, z_1) \tag{38}$$

in a quark jet, and

$$\mathcal{N}_g^q(Q_0, Q) = \frac{8}{3}\frac{n_f}{b}\tilde{\mathcal{N}}(z_0, z_1) \tag{39}$$

in a gluon jet, where

$$z_0 = \sqrt{\frac{32\pi C_A}{b^2\alpha_s(Q_0)}}, \tag{40}$$

$$z_1 = \sqrt{\frac{32\pi C_A}{b^2\alpha_s(Q)}}, \tag{41}$$

$$\mathcal{N}^-(z_0, z_1) = \left(\frac{z_0}{z_1}\right)^{\frac{8}{3}\frac{C_F}{C_A}\frac{n_f}{b}}, \tag{42}$$

$$\tilde{\mathcal{N}}(z_0,z_1) = \left(\frac{z_0}{z_1}\right)^B [I_B(z_1)K_B(z_0) - K_B(z_1)I_B(z_0)], \quad (43)$$

$$B = \left(\tfrac{11}{3}C_A + \tfrac{2}{3}n_f - \tfrac{4}{3}n_f\frac{C_F}{C_A}\right)/b, \quad (44)$$

$$b = \tfrac{11}{3}C_A - \tfrac{2}{3}n_f, \quad (45)$$

and I_B, K_B are the modified Bessel functions of order B. We shall also be making use of the function

$$\mathcal{N}^+(z_0,z_1) = z_1\left(\frac{z_0}{z_1}\right)^B [I_{B+1}(z_1)K_B(z_0) + K_{B+1}(z_1)I_B(z_0)], \quad (46)$$

which determines the diagonalised parton multiplicity to next-to-leading logarithmic accuracy[3], and thus gives the leading contribution to the gluon multiplicity in a jet[4]. We obtain the heavy quark pair multiplicities as

$$\mathcal{N}_q^{Q\bar{Q}}(Q_0,Q) = \left(\mathcal{N}_q^q(Q_0,Q) - 1\right)/2n_f, \quad (47)$$

$$\mathcal{N}_g^{Q\bar{Q}}(Q_0,Q) = \mathcal{N}_g^q(Q_0,Q)/2n_f, \quad (48)$$

with

$$Q_0 = 2m_q, \quad (49)$$

$$n_f = q. \quad (50)$$

Note that $\tilde{\mathcal{N}}$ contributes next-to-leading logarithmic terms (i.e. terms of the form $\alpha_s^n L^m$, $m = 2n-1$, $L = \log(Q/Q_0)$), while $\mathcal{N}^-$ has a power series in $\alpha_s L$, only the first two terms of which contribute at next-to-leading logarithmic accuracy. Note also that at asymptotically large scales, $\mathcal{N}^-$ is negligible relative to $\tilde{\mathcal{N}}$ and the heavy quark multiplicity in a quark jet is the same as that in a gluon jet, scaled down by a factor C_F/C_A. As we have already seen from the Monte Carlo algorithm, this is far from the case at current or foreseeable energy scales, where the multiplicity in quark jets is considerably suppressed relative to that in gluon jets. Near threshold, the pair multiplicities have the following expansions (the threshold region is formally defined as the region where $\alpha_s L^2 \ll 1$ but $L \gg 1$),

$$\mathcal{N}_g^{Q\bar{Q}}(Q_0,Q) = \frac{\alpha_s}{4\pi}\left\{\tfrac{4}{3}L\right\} + \left(\frac{\alpha_s}{4\pi}\right)^2\left\{\tfrac{16}{9}C_A L^3 - \tfrac{4}{3}b(B+1)L^2\right\} + \mathcal{O}(\alpha_s^3), \quad (51)$$

$$\mathcal{N}_q^{Q\bar{Q}}(Q_0,Q) = \left(\frac{\alpha_s}{4\pi}\right)^2\left\{\tfrac{16}{9}C_F L^3 - \tfrac{4}{3}\frac{C_F}{C_A}(11C_A - \tfrac{8}{3}\frac{C_F}{C_A}n_f - \tfrac{2}{3}n_f)L^2\right\} + \mathcal{O}(\alpha_s^3). \quad (52)$$

When we are even closer to threshold, $L \to 0$, the logarithmic terms are no longer dominant, and one should add the process-dependent non-logarithmic terms from a fixed order calculation[4]. Thus the above expressions are not relevant in that limit. Nevertheless, it would be convenient if the expressions we use are at least

reasonably behaved there. It can be seen that this is the case for gluon jets, since (51) rises linearly for L close to zero. However, for quark jets, since the $\mathcal{O}(\alpha_s)$ term is missing, the leading term in (52) is a quadratic fall to negative values, which is clearly undesirable. Since this term is of the form $\alpha_s^n L^m$, $m < 2n-1$, it is beyond the scope of a next-to-leading log calculation and is completely undetermined. Note that the coefficients of α_s^n in (51) and (52) terminate at $m = n$, i.e. there are no terms in $\alpha_s^n L^m$, $m < n$, so the quadratic behaviour in L is entirely given by the $\alpha_s^2 L^2$ term.

We can use the fact that this region is undetermined to alter the expression to a more physically reasonable form. Indeed, as mentioned earlier, $\mathcal{N}^-$ does not generate any relevant logarithms beyond the first order, and so it can be replaced by any function $\tilde{\mathcal{N}}^-((z_1/z_0)^2)$ having the properties

1. $\tilde{\mathcal{N}}^-(x) \to 1 - \frac{4}{3}\frac{C_F}{C_A}\frac{n_f}{b}(x-1)$ as $x \to 1$,
2. $\tilde{\mathcal{N}}^-(x) \to 0$ as $x \to \infty$.

We arbitrarily decide to define $\tilde{\mathcal{N}}^-(x)$ in such a way that the $\alpha_s^2 L^2$ term in $\mathcal{N}_q^{Q\bar{Q}}$ is exactly zero. This corresponds to modifying condition 1,

1'. $\tilde{\mathcal{N}}^-(x) \to 1 - \frac{4}{3}\frac{C_F}{C_A}\frac{n_f}{b}(x-1) + \frac{2}{3}\frac{C_F}{C_A}\frac{n_f}{b}(B+1)(x-1)^2$ as $x \to 1$.

One such function is

$$\tilde{\mathcal{N}}^-(x) = \mathcal{N}^-(x)\left(1 + \alpha(x-1)^2 e^{-2(x-1)}\right), \quad (53)$$

$$\alpha = \tfrac{2}{3}\frac{C_F}{C_A}\frac{n_f}{b}\left(B - \tfrac{4}{3}\frac{C_F}{C_A}\frac{n_f}{b}\right). \quad (54)$$

Note that for $n_f = 5$, $\alpha \approx 0.2$, which implies that $\tilde{\mathcal{N}}^-$ is never more than about 3% above $\mathcal{N}^-$. We stress that no special significance is claimed for this particular form of $\tilde{\mathcal{N}}^-$; within the next-to-leading logarithmic approximation in which it is valid, it is identical to $\mathcal{N}^-$. It does however ensure that $\mathcal{N}_q^{Q\bar{Q}}$ is a positive quantity for all $L > 0$.

An alternative approach was taken in [5], where the heavy quark pair multiplicities were obtained by explicit integration of the gluon multiplicities,

$$\mathcal{N}_c^{Q\bar{Q}}(Q_0,Q) = \tfrac{1}{3}\int_{Q_0}^{Q}\frac{dk}{k}\frac{\alpha_s(k^2)}{\pi}\left(1 + \frac{Q_0^2}{2k^2}\right)\sqrt{1 - \frac{Q_0^2}{k^2}}\,\mathcal{N}_c^g(k,Q), \quad c = q,g. \quad (55)$$

Note that this includes terms that are power-suppressed relative to the next-to-leading log results. However, the first of these is $\sim (Q_0/k)^4$ so we do not expect

it to contribute significantly. Neglecting the power-suppressed terms, this can be written in terms of the variables introduced earlier, as

$$\mathcal{N}_c^{Q\bar{Q}}(z_0, z_1) = \frac{4}{3b}\int_{z_0}^{z_1} \frac{dz}{z}\mathcal{N}_c^g(z, z_1), \tag{56}$$

which can be integrated using the results

$$\int_{z_0}^{z_1} \frac{dz}{z}\mathcal{N}^+(z, z_1) = \frac{z_1}{z_0}\tilde{\mathcal{N}}(z_0, z_1) + \ldots, \tag{57}$$

$$\int_{z_0}^{z_1} \frac{dz}{z}\mathcal{N}^-(z, z_1) = \frac{3}{8}\frac{C_A}{C_F}\frac{b}{n_f}\left(1 - \mathcal{N}^-(z_0, z_1)\right), \tag{58}$$

$$\int_{z_0}^{z_1} \frac{dz}{z}\tilde{\mathcal{N}}(z, z_1) = \frac{1}{z_0 z_1}\mathcal{N}^+(z_0, z_1) + \ldots, \tag{59}$$

where the neglected terms in (57) and (59) are suppressed by additional factors of $z_{0,1}$. Since $\mathcal{N}^+$ is leading, and $\tilde{\mathcal{N}}$ is next-to-leading, the neglected terms of (57) and the whole of (59) result in only sub-leading logarithms and can be neglected. Then, given the gluon multiplicities in [4], one obtains the same expressions for the heavy quark pair multiplicities as given in (47,48), except that both occurrences of $\tilde{\mathcal{N}}$ are multiplied by an extra factor of z_1/z_0. Since $\tilde{\mathcal{N}}$ only generates next-to-leading logarithms, and z_1/z_0 has the expansion

$$\frac{z_1}{z_0} = 1 + \frac{b}{\pi}\alpha_s L + \ldots, \tag{60}$$

the extra factor makes no difference to next-to-leading logarithmic accuracy, and the two approaches are identical. This shows that the exponent of the coefficient in (43) is undetermined to this accuracy*. These differences can be used as a rough guide to the importance of sub-leading logarithms, and of power-suppressed terms.

In Fig. 5 we show the multiplicity of bottom quark pairs in a gluon jet, according to each of these approaches, together with the results from HERWIG. The solid curves are the direct next-to-leading logarithmic approach for two different values of Λ. Recall that the next-to-leading logarithmic approximation contains no renormalisation-scheme dependence, so Λ is considered a free parameter, unrelated to $\Lambda_{\overline{MS}}$. The dot-dashed curve is the integral of the gluon multiplicity, neglecting the power-suppressed terms. The difference between this and the solid curve is purely because of the sub-leading logarithmic terms, and gives a rough indication of their size, which is small. Finally the dashed curve is the full integral, including the power-suppressed terms, which are also seen to be small, even

*The inconsistency between the two methods is because of the asymmetry in [4] between the treatment of the two scales Q and Q_0. One would expect the integration method to give a better estimate of the exponent's value[14]

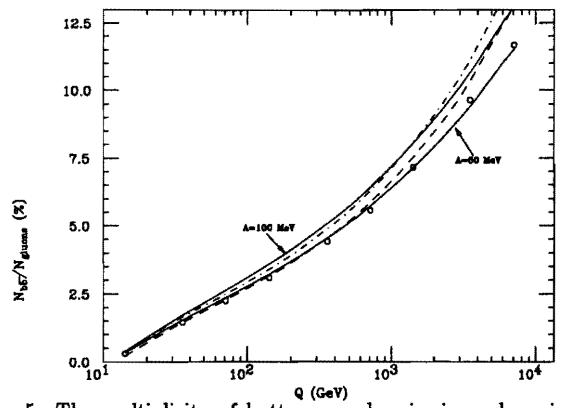

Figure 5: The multiplicity of bottom quark pairs in a gluon jet as a function of the jet hardness, Q, using the explicit next-to-leading logarithmic expressions (solid), the integrated gluon multiplicity (dashed), and the latter neglecting power-suppressed terms (dot-dashed). All curves use $\Lambda = 100$ MeV, except the solid ones, which use the values shown. The points are from the Monte Carlo algorithm.

for Q not too far above threshold. Both of these effects are smaller than variation of the unknown parameter Λ. We conclude that using the next-to-leading logarithmic approximation alone to predict the heavy quark multiplicity in a gluon jet is reasonably reliable. We also see that the Monte Carlo results are in reasonable agreement with the next-to-leading logarithmic approximation.

In Fig. 6 we show the equivalent for quark jets, which is not so reassuring. The problem of the negative threshold extends to well over 100 GeV, and the sub-leading terms that were added to solve it still make a significant difference for Q well over 1 TeV. Furthermore the sub-leading terms indicated by the difference between the direct and integrated methods are also large. These problems are all because of the suppression of the leading terms in the threshold region, which exaggerates the importance of sub-leading corrections. We conclude that the next-to-leading logarithmic approximation alone is not a good way to predict the heavy quark multiplicity in a quark jet at current or foreseeable energies, and it needs to be augmented with the process-dependent non-logarithmic terms. This is not too severe a problem for practical calculations, as the production of high-p_t heavy quark pairs in hadron-hadron collisions is dominated by gluon jets.

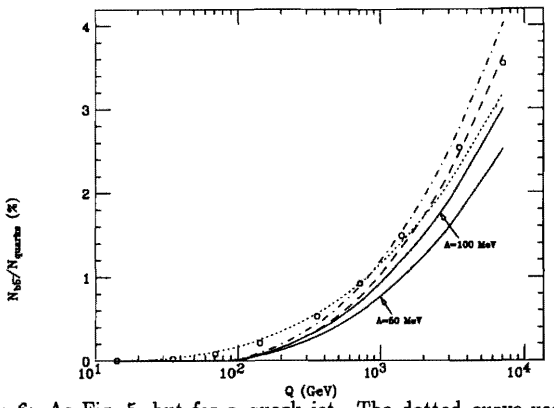

Figure 6: As Fig. 5, but for a quark jet. The dotted curve uses the modified result from Eq. 53.

4 Hadron-hadron Collisions

When simulating the general hard processes relevant to hadron-hadron collisions, one encounters several effects in addition to those discussed above for colour-singlet sources. Since the incoming partons are coloured, they are able to emit gluons. Recoil from this emission means that the hard process cmf acquires a transverse momentum, p_t, relative to the hadron-hadron cmf. The singularities of the matrix element are manifested in the p_t spectrum as a singularity as $p_t \to 0$, and it is essential that the corresponding logarithms are resummed to all orders to provide a finite p_t spectrum. This can be done using a Monte Carlo algorithm known as backward evolution[15], which evolves the incoming parton downward in scale from the hard interaction back into the incoming hadron. This can also be formulated to resum the soft logarithms by careful choice of the evolution variable[7], at least in the region where x is not too small.

The hard interaction plays two rôles: in defining the kinematics of the hard jets of the event, and in defining the initial conditions for the evolution of the incoming and outgoing partons. Coherence effects are particularly important for the latter[7], which limit soft gluon emission from a given a parton to an angular cone defined by the opening angle to its 'colour connected' partner. The idea of colour connectedness is only well defined in the large-N_c limit, but the additional terms, which are both colour-suppressed and dynamically suppressed, can be distributed amongst the leading terms in such a way that each sub-process cross-section is a positive quantity throughout phase-space[7].

There are four separate sources of heavy quarks in hadron-hadron collisions:

1. Pair production;
2. Flavour excitation;
3. Final-state parton evolution; and
4. Initial-state parton evolution.

Throughout the following we consider the first two together, as the hard process contribution. The separation is entirely arbitrary, and the description of the entire process, i.e. the sum of all four, should not depend on it. A crucial rôle in this separation is played by the factorisation scale μ, since particle production above this scale is attributed to the hard interaction, while that below it is attributed to the parton evolution. In HERWIG, since we only use the lowest order expression for the hard scattering, this is easily defined as

$$\mu^2 = \frac{2stu}{s^2+t^2+u^2} \sim p_t^2, \tag{61}$$

in the case of massless $2 \to 2$ scattering, and

$$\mu^2 = \frac{2s(t-m_q^2)(u-m_q^2)}{s^2+(t-m_q)^2+(u-m_q)^2} \sim m_t^2, \tag{62}$$

in the massive case, where the transverse mass m_t is given by $m_t^2 = p_t^2 + m_q^2$. Thus it is essential for a complete description, that all emission within the parton evolution be at scales below this, in addition to the limits imposed by colour coherence. In the standard algorithm, this is simple to implement—if a gluon emission with local transverse momentum above μ, or gluon splitting with transverse mass above μ is generated, then it is vetoed and evolution continues from the generated scale. However, since this modifies the form factor in a way that cannot be easily calculated, it means that we cannot use it when forcing heavy quark production.

To be explicit, the problem is the following; if we are to force a $g \to q\bar{q}$ splitting, then the associated weight factor must include the probability that there was not a $g \to gg$ splitting at a larger scale. Although we know the probability that such a splitting was not generated, since this is just the form factor, we do not know the fraction of generated splittings that would have been rejected, eventually resulting in no emission. Thus we cannot switch off any type of branching in a region in which it could get vetoed (except in cases where the corresponding effective form factor can be explicitly calculated).

This veto is only active in collisions in which the two outgoing partons have a rapidity difference of ~ 3.4 or more, because of the hard process kinematics and

the colour coherence condition. Since in the following we will require the detected heavy quarks to be reasonably central, the recoiling jet must be at large rapidity in order for any vetoes to be possible. Thus only a small fraction of hard scatters leads to jets that could require a veto. Even in those cases, since the scale of the jet is not too far above the threshold for vetoing, the fraction of emissions in the 'veto region' (the range of Q^2 where a veto is possible) is small.

The strategy we adopt is therefore as follows. If we are required to force an emission in a jet that is above this threshold, it is allowed to evolve naturally through the veto region. If this gives no emission within the region, then the forcing algorithm is used as normal, starting immediately below the veto region. If it happens to give the parton that was intended to be forced, then the forcing algorithm continues as normal. If it gives any other parton, then the event is given zero weight. In this way, such jets are simulated correctly, even though the Monte Carlo efficiency is not as good as in the usual case. It can be immediately seen that if the veto region covered the whole of phase-space, this would reduce to the standard method of jet evolution, and the forcing algorithm would not be used. Thus a forcing algorithm cannot be used in Monte Carlo programs in which vetoes are prevalent.

Having implemented such an algorithm, it is straightforward to study any desired quantity. As an example, we show in Fig. 7 the p_t spectrum of $b\bar{b}$ pairs in $p\bar{p}$ collisions at 1.8 TeV. Experimentally bottom quarks must be reasonably central to be detected, so we make a representative cut of $|\eta| < 1$ for both the quark and antiquark. The spectrum peaks at around $2m_b$, as would be expected. Also shown are the equivalent curves for various ranges of p_t of the hard process. Although this is not a directly measurable quantity, similar results would be obtained by, for example running a jet algorithm on the event, and cutting on the p_t of the hardest jet on the opposite side to the $b\bar{b}$ pair. It can be seen that for each range of hard process p_t, the $b\bar{b}$ p_t peaks at about the bottom of the range, meaning that the pair takes most of the jet energy on average. There are also considerable tails above and below the selected range, owing to recoil from the other jets in the event and (in the latter case) to pairs that take considerably less than the whole jet energy.

In Fig. 8, the spectrum is shown again, in comparison with that from the hard process. Although this has a larger cross-section, it falls more rapidly with p_t than the production in jets does, since this p_t is predominantly recoil from the initial-state radiation, which is constrained to be less than the factorisation scale, $\mu \sim m_t$. The m_t spectrum is dominated by the region close to m_b, so the pair p_t falls rapidly above this value. The total cross-section from the hard process is about three times larger than that from jets, and so the latter is an important correction. For large pair transverse momenta, $p_t \gtrsim 30$ GeV, the latter

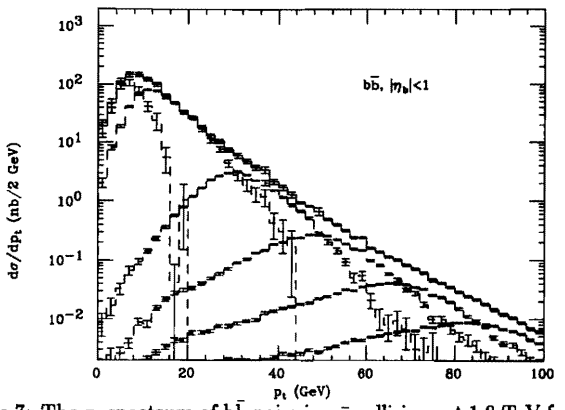

Figure 7: The p_t spectrum of $b\bar{b}$ pairs in $p\bar{p}$ collisions at 1.8 TeV from production in jets (solid). Also shown (dashed) are the individual contributions from events in which the hard process p_t, measured in GeV, is in the range (from left to right), $p_t < 10$, $10 < p_t < 30$, $30 < p_t < 50$, $50 < p_t < 70$, $70 < p_t < 90$, and $p_t > 90$. The errors shown are purely statistical.

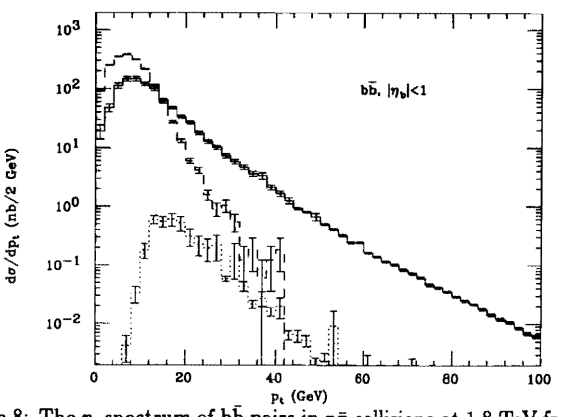

Figure 8: The p_t spectrum of $b\bar{b}$ pairs in $p\bar{p}$ collisions at 1.8 TeV from production in jets (solid), from the hard process (dashed), and the leading contribution from initial-state radiation (dotted).

is completely dominant.

As stressed earlier, to describe the whole process all the possible sources of heavy quark pairs must be included, but we have so far neglected the possibility of them being created during the initial-state evolution. There are two ways in which this can happen, either by a gluon being evolved backwards into a heavy quark, or by the emission of a gluon that splits into a heavy quark pair. We expect the former to be negligible, owing to the smallness of the distribution functions for heavy quarks at currently attainable scales. We would expect the latter to behave in a similar way to the final-state quark jet case, i.e. to be formally of the same logarithmic order as from final state gluon jets, but considerably suppressed near threshold by the requirement that a gluon is emitted at a large enough scale to contain the heavy quark pair. Although we have not developed a forcing algorithm that systematically sums all such configurations, we can estimate its size by forcing its leading contribution—the hardest gluon emitted producing a heavy quark pair at its first branching. This is also shown in Fig. 8, and is negligible at around one percent of the final-state contribution. We therefore feel justified in neglecting the possibility of initial-state production at present.

We conclude that the production of heavy quark pairs in final-state jets is an important component of the total cross-section for bottom quarks in hadron-hadron collisions. Furthermore it is an essential component of any study that involves pairs produced with transverse momenta more than a few times the bottom quark mass. The background to the top quark search is one such example. We have implemented a forcing algorithm that allows such production to be studied in a reasonable amount of computer time, unlike previous algorithms that produce heavy quark pairs with the same frequency as in nature. The results of the algorithm are in good agreement with analytical results in the next-to-leading logarithmic approximation, at least for the physically important case of gluon jets. For quark jets, the analytical results are not reliable without the addition of process-specific non-logarithmic terms.

Acknowledgments

I am grateful to Bryan Webber and Yuri Dokshitzer for many helpful discussions of these and related topics.

References

1. A.H. Mueller and P. Nason, Phys. Lett. 157B (1985) 226.
2. A.H. Mueller and P. Nason, Nucl. Phys. B266 (1986) 265.
3. Yu.L. Dokshitzer, V.A. Khoze, A.H. Mueller and S.I. Troyan, *Basics of Perturbative QCD*, Editions Frontières, Gif-sur-Yvette, 1991.
4. S. Catani, Yu. Dokshitzer, F. Fiorani and B.R. Webber, Nucl. Phys. B377 (1992) 445.
5. M.L. Mangano and P. Nason, Phys. Lett. 285B (1992) 160.
6. G. Marchesini and B.R. Webber, Nucl. Phys. B238 (1984) 1.
7. G. Marchesini and B.R. Webber, Nucl. Phys. B310 (1988) 461.
8. G. Marchesini, B.R. Webber, G. Abbiendi, I.G. Knowles, M.H. Seymour and L. Stanco, Computer Phys. Comm. 67 (1992) 465.
9. T. Sjöstrand, Computer Phys. Comm. 46 (1987) 367.
10. Yu.L. Dokshitzer, Phys. Lett. 305B (1993) 295.
11. B.R. Webber, Nucl. Phys. B238 (1984) 492.
12. B. Andersson, G. Gustafsson, G. Ingelman and T. Sjöstrand, Phys. Rep. 97 (1983) 33.
13. S. Catani, G. Marchesini and B.R. Webber, Nucl. Phys. B349 (1991) 635.
14. Yu.L. Dokshitzer, private communication.
15. T. Sjöstrand, Phys. Lett. 157B (1985) 321.